

# Optimizing growth conditions for BiMnO<sub>3</sub>

C. Morien

July 29, 2008

## Abstract

The growth conditions for thin-film BiMnO<sub>3</sub> on SrTiO<sub>3</sub>(001) substrate were optimized by altering the substrate temperature and oxygen partial pressure during growth. BiMnO<sub>3</sub> thin films were grown using pulsed laser deposition. The samples were characterized using x-ray diffraction, resistivity measurements, and magnetization measurements. The optimal substrate temperature was found to be 620 °C, and the optimal oxygen partial pressure was found to be 25 mTorr. These conditions led to a T<sub>C</sub> of 93 K and a coercive field of 420 Oe.

## 1 Introduction

BiMnO<sub>3</sub> is a multiferroic material, which means it exhibits both ferromagnetism and ferroelectricity. A ferromagnet is a material that becomes magnetized in the presence of an external magnetic field, and retains that magnetization even after the external field has been removed. A ferroelectric is a material that exhibits electrical polarization, analogous to the spontaneous magnetization of a ferromagnet, that can be switched by the application of an external electric field.

Bismuth manganese oxide is not stable at atmospheric pressure, requiring pressures of approximately 6 GPa and temperatures of approximately 1100 K to fabricate in bulk [1]. These extreme conditions are overcome by depositing thin films of BiMnO<sub>3</sub> using pulsed laser deposition (PLD) onto a substrate with similar lattice spacing. The substrate on which BiMnO<sub>3</sub> is grown is SrTiO<sub>3</sub>(001) (STO). The (001) indicates that the film grows along the top face of the substrate's unit cell structure, as opposed to along the diagonal.

STO has a cubic structure with a lattice spacing of 3.905 Å; BiMnO<sub>3</sub> has a monoclinic unit cell, best described as a triclinically distorted perovskite cell with a lattice spacing in

the  $a$  and  $c$  direction of  $3.935 \text{ \AA}$  and a lattice spacing in the  $b$  direction of  $3.989 \text{ \AA}$ . This gives a lattice mismatch of  $0.77 \%$  on the  $a$  and  $c$  axis and  $2.15 \%$  on the  $b$  axis [2]. A minimal lattice mismatch is desirable because it will reduce strain within the deposited thin film. Since strain can alter the properties of a multiferroic, a large lattice mismatch, and thus a large strain, will alter the thin film's properties and prevent accurate analysis. A perovskite usually has an  $ABO_3$  structure, as is true of  $\text{BiMnO}_3$ , and is a body centered cubic unit cell with the 'A' atoms at the body center, the 'B' atom at the corners, and the oxygen atoms at the bond centers, as shown in Figure 1.

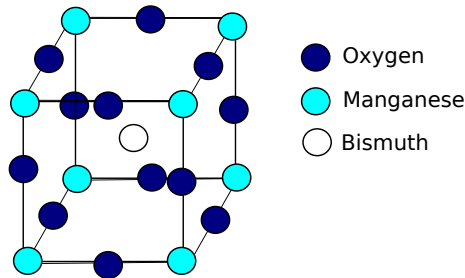


Figure 1: Perovskite structure of  $\text{BiMnO}_3$ .

This report describes the optimization of the growth conditions for multiferroic thin films of  $\text{BiMnO}_3$  by altering the temperature and oxygen partial pressure during growth and then characterizing the films. Training for the required techniques was done by growing and analyzing thin films of  $\text{L}_{0.5}\text{P}_{0.5}\text{CaMnO}_3$  (LPCMO). The optimal growth conditions for LPCMO are well known, making it an easy sample to train with.

In PLD, a laser beam is directed at a solid target with a composition similar to that of the desired film. The interaction between the laser and target causes the top layer of the target to vaporize and form a plume of material that is projected outward normal to the target. The vaporized material travels toward a heated substrate, where it condenses and forms a thin film. The substrate temperature is a condition that must be optimized and was varied between  $500 \text{ K}$  and  $715 \text{ K}$ . The deposition occurs in the presence of  $\text{O}_2$  background

gas in order to fully oxygenate the deposited film, as well as to prevent the volatile Bi from escaping the sample. The  $O_2$  partial pressure is another condition that must be optimized and was varied between 25 and 100 mTorr.

Two important properties of ferromagnets and multiferroics are the Curie temperature,  $T_C$ , and the coercive field. The Curie temperature is the temperature above which a ferromagnet no longer exhibits ferromagnetism. Above this temperature the material acts like a paramagnet, exhibiting a magnetic moment *only* in the presence of an external magnetic field. The coercive field refers to the strength of the magnetic field that must be applied to a saturated ferromagnet in order to reduce the magnetization to zero. A ferromagnet is saturated when any additional external magnetic field will produce only negligible changes in the magnetic flux density. For thin films of  $BiMnO_3$  grown under optimal conditions, the  $T_C$  should be near 100 K and the coercive field should be near 500 Oersteds (Oe). An Oe is a unit of magnetizing field strength.

The  $T_C$  and coercive field are determined from magnetization measurements made using a superconducting quantum interference device (SQUID). The SQUID is an extremely sensitive magnetometer, which can measure extremely small fields on the order of  $10^{-18}$  T. Measuring the magnetic moment with a changing applied field produces a hysteresis loop when the sample is ferromagnetic. Figure 2 illustrates a hysteresis loop and indicates significant features. The x-axis is the external magnetic field (Oe), and the y-axis is the flux density (emu), where emu is electromagnetic units. Electromagnetic units are the CGS unit of magnetization. This unit can be converted into units of Bohr magnetons ( $\mu_B$ ), which give a good indication of the degree of magnetization in the material. The retentivity is the residual magnetic field retained by the magnet when the external magnetic field has been removed. The coercivity is the field value where the hysteresis curve crosses the x-axis. Analyzing the data produced from measuring the magnetic moment with a changing temperature yields the  $T_C$ .

The coupling between ferromagnetism and ferroelectricity in multiferroics leads to a mag-

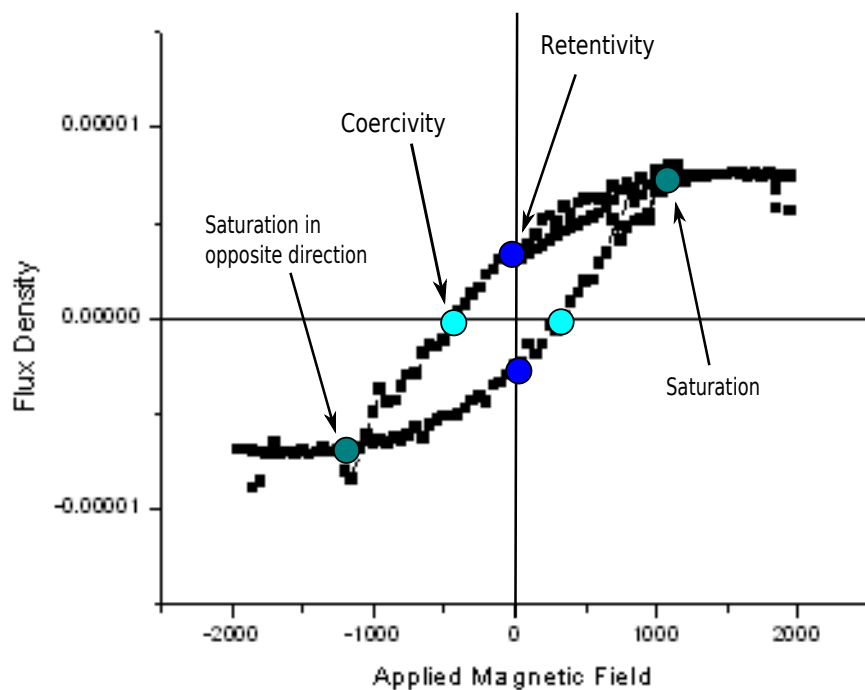


Figure 2: An example of a hysteresis loop showing the retentivity, coercivity, and saturation points. The x-axis is the external applied field ( $H$ ), and the y-axis is the flux density of the sample ( $B$ ).

netic polarization that can be switched with the application of an electric field, and a ferroelectric polarization that can be switched with the application of a magnetic field. This property is of great technological interest [3]. A notable application of magnetoelectric coupling in multiferroics is in digital data storage. The storage of electronic information in the electric polarization state of a ferroelectric material has already been implemented. A drawback to this technology, which has limited its realization, is the necessity for destructive readout, which severely decreases the reliability and lifetime of ferroelectric memories. A ferroelectric capacitor used to store a bit of memory must be “read” by applying a voltage to the capacitor and measuring the current through a resistor in series in comparison to a reference cell [4]. The application of voltage across the capacitor changes its state, forcing the memory to be rewritten after each read operation. This extra write operation causes the capacitor to fatigue more quickly and hastens device failure. The use of a multiferroic material in digital data storage would allow memory to be written electronically and

read magnetically, eliminating the destructive readout and increasing device reliability and lifetime.

## 2 Training

I trained in PLD techniques by growing thin films of LPCMO, which were deposited on 10-mm  $\times$  10-mm substrates of NdGaO<sub>3</sub> (NGO). Optimal growth conditions for LPCMO are well known. I grew the LPCMO films in an oxygen atmosphere with a partial pressure of 450 mTorr and a substrate temperature of 820 °C heated at a rate of 20 °C/min. I performed Pre-ablation for 5 min, and deposition occurred for 8 min. The oxygen partial pressure during cool down was 450 Torr. Fig. 3 shows the plume produced by the ablation of LPCMO. Further explanation of PLD techniques will be provided in Section 3.

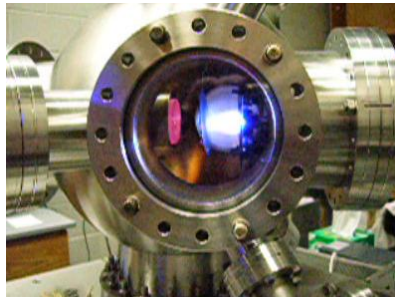


Figure 3: Plume produced from the ablation of LPCMO within the vacuum chamber.

I used a 9-T superconducting magnet system from American Magnetics to measure the resistance of the LPCMO samples over a range of temperatures. The temperature was regulated with a Janis SuperVaritemp insert. A plot of sheet resistance versus temperature is shown in Fig. 4. This plot indicates that a metal to insulator transition exists near 127 K as the temperature is ramped up, and a insulator to metal transition occurs near 110 K as the temperature is ramped down. This is the expected behavior of LPCMO, which has both metallic and insulating phases. Further explanation of resistivity measurement techniques will be provided in Section 4.3

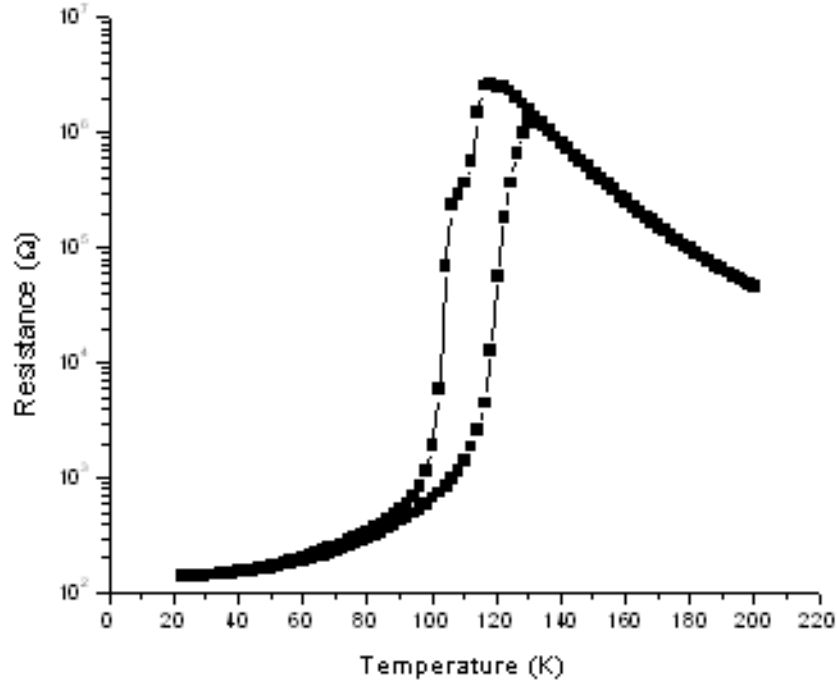


Figure 4: Sheet resistance vs temperature for LPCMO sample 061108a.

### 3 Thin Film Growth of $\text{BiMnO}_3$

I performed the ablation with a Lambda Physik KrF excimer laser ( $\lambda = 248 \text{ nm}$ ) at an energy of approximately 480 mJ and a frequency of 5 Hz. The composition of the target was  $\text{Bi}_{2.4}\text{MnO}_3$ , which is similar to the desired composition of the film. An excess of Bi is used because Bi is volatile. The laser struck the rotating target at an angle, which sent a plume of vaporized material normal to the surface of the target and onto the heated substrate. See Fig. 5.

I grew thin films of  $\text{BiMnO}_3$  using PLD using a  $\text{Bi}_{2.4}\text{MnO}_3$  target on a  $5\text{-mm} \times 5\text{-mm}$  substrates of STO(001). The films were grown in an atmosphere of oxygen, and the partial pressure was varied between 25 and 100 mTorr. I varied the temperature of the substrate between 500 and 750 °C, heated at a rate of 20 °C/min. Pre-ablation was performed for 5 min to clean the target, and deposition time varied between 20 and 40 min. The oxygen partial pressure during cool down was 760 torr. Figure 5 shows the plume produced by

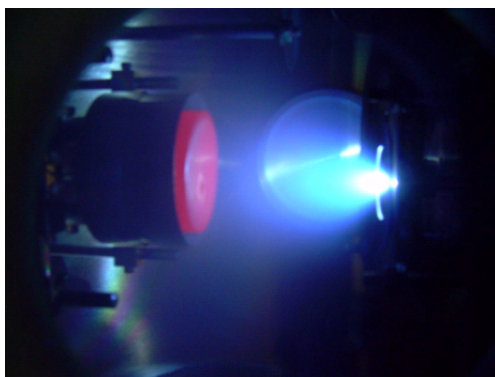


Figure 5: Plume produced from the ablation of  $\text{BiMnO}_3$  within the vacuum chamber. The substrate and heating unit are glowing red on the left side, and the plume in blue is on the right side. Color may not be visible in printed version.

ablation of the  $\text{Bi}_{2.4}\text{MnO}_3$  target. Refer to Table 1 for a complete list of parameters for the the films grown for this project.

## 4 Thin Film Characterization

### 4.1 X-ray Diffraction

Previous x-ray diffraction measurements performed on samples made by another student prior to this project indicated the presence of  $\text{BiMnO}_{3+x}$  only in sample 022508a, with the  $\text{BiMnO}_3$  peak at approximately  $42^\circ$ . Sample 022508a was grown at a temperature of  $450^\circ\text{C}$ , while the three remaining samples were grown at temperatures at or above  $690^\circ\text{C}$ . The presence of  $\text{BiMnO}_{3+x}$  in only the low temperature sample suggests that a different configuration of Bi, Mn, and O is deposited at higher temperature or the substrate temperature may have been too high to condense the volatile Bi cations. Thus, we have found that  $\text{BiMnO}_3$  is only deposited at lower temperatures. For this reason all samples in this project were grown below  $650^\circ\text{C}$ .

X-ray diffraction measurements for sample 071508a and the pure STO substrate are shown in Figure 6. The 002 STO peak appears at approximately  $47^\circ$  and the  $\text{BiMnO}_3$  peak appears at  $45^\circ$ . Published literature indicates the  $\text{BiMnO}_3$  peak should be located at

Table 1: Growth parameters for BiMnO<sub>3</sub> thin films. All films were heated at a rate of 20°C/min, with a pre-ablation time of 5 min, a laser energy of 480 mJ, a laser frequency of 5 Hz, grown in an atmosphere of O<sub>2</sub>, and cooled down with a partial pressure of 760 torr.

\* Grown prior to this project by another student, but included for completeness.

Sample Name	O <sub>2</sub> Partial Pressure (mTorr)	Substrate Temperature (°C)	Deposition Time (min)
010708a *	20	715	10
013008a *	20	690	20
013108a *	20	715	20
022508a *	20	450	16
061908a	25	500	20
062008a	25	550	20
062508a	26	550	40
062608a	26	600	40
062708a	26	650	40
070108a	100	550	40
070208a	100	600	40
070308a	100	650	40
071508a	25	620	40
071608a	25	580	40

approximately 45.5°, with the 002 STO substrate peak at approximately 46.5°. Samples grown in both 25 mTorr and 100 mTorr oxygen partial pressures were tested. We conclude that the optimal partial pressure likely lies between these two values, and further depositions at smaller increments must be performed to determine the optimal partial pressure.

A potential method for enhancing the presence of BiMnO<sub>3</sub> is post-annealing, in which the sample is placed in a furnace after it has been grown. Due to the volatile nature of Bi, the post-annealing would need to take place in an atmosphere of oxygen. This approach has not yet been implemented because it would introduce additional variables, such as annealing temperature and oxygen partial pressure, to the growth process. Once the present method has been optimized, it may be desirable to try post-annealing.

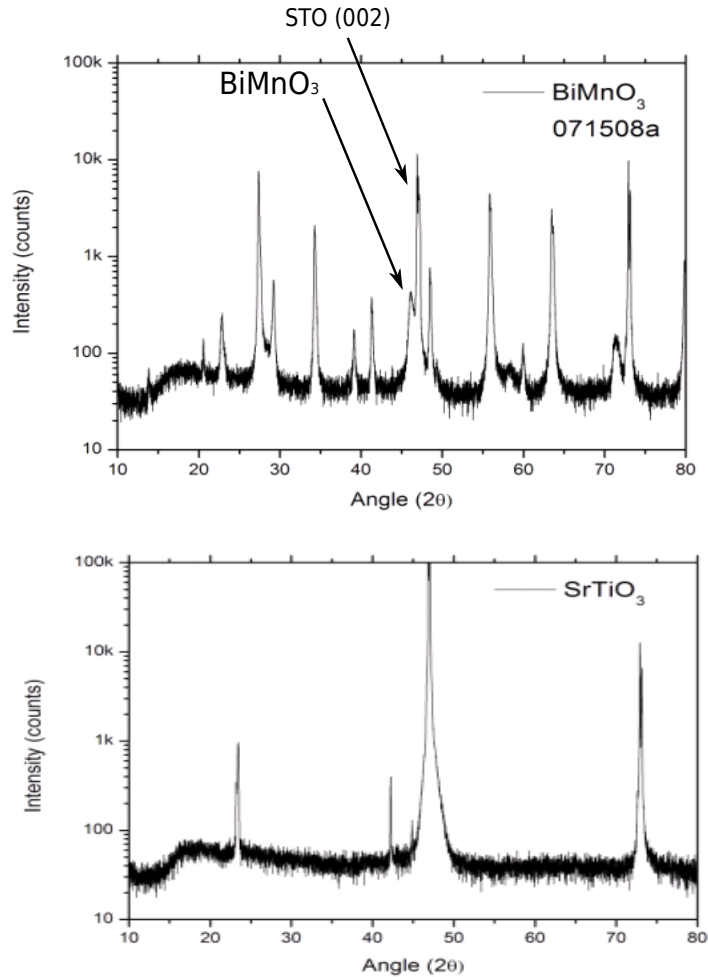


Figure 6: X-ray diffraction measurements for sample 071508a and a pure substrate, showing the peaks for the STO substrate and the  $\text{BiMnO}_3$  thin film.

## 4.2 SQUID

A SQUID magnetometer was used to measure the magnetic moment of the samples with respect to temperature and with respect to external magnetic field. The MPMS Multivu software was used to generate sequences. See Appendix A for an example of the sequence used for our measurements. Measuring the magnetic moment of the sample with respect to changing temperature generates an  $M$  vs  $T$  ( $M$ - $T$ ) curve, which can be used to determine the  $T_C$  of the sample. Measuring the magnetic moment of the sample with respect to changing external field generates an  $M$  vs  $H$  ( $M$ - $H$ ) curve, which can be used to determine the coercive

field of the sample.

I took M-T measurements at 500 Oe. I then performed scans from 10 to 200 K and then again from 200 to 10 K. M-H measurements were taken at a range of temperatures from 10 to 120 K in 10 K increments. I took the scans at each respective temperature from 0 to 2000 Oe, then from 2000 to -2000 Oe, and finally from -2000 to 2000 Oe. The increments were smaller near the center of the hysteresis loop and larger around the edges. The field was then returned to 0 Oe before beginning the scan at the next temperature.

Figure 7 shows the M-H curve for sample 071508a of  $\text{BiMnO}_3$ , taken at 10 K from -2000 to 2000 Oe in varying increments. The point where the curve crosses the x-axis is the coercivity. The coercive field is determined by averaging the absolute values of the negative and positive field values. The coercive field for the pictured sample at 10 K is 420 Oe.

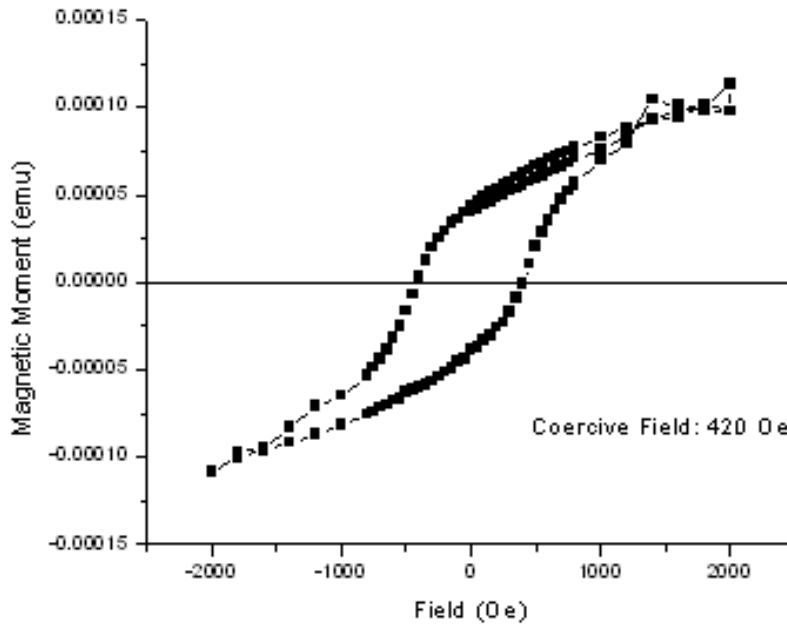


Figure 7: M-H loop at 10 K for sample 071508a of  $\text{BiMnO}_3$ , showing a coercive field of 420 Oe.

Fig. 8 shows the M-T curves for samples 062608a and 062708a of  $\text{BiMnO}_3$  and sample 010708a, which is not believed to be  $\text{BiMnO}_3$  but rather some other manganite. The  $T_C$  is indicated by the point at which the magnetic moment drops suddenly, resulting from the

sample becoming paramagnetic. The drop for sample 010708a is extremely steep and can be seen to be 48 °C.

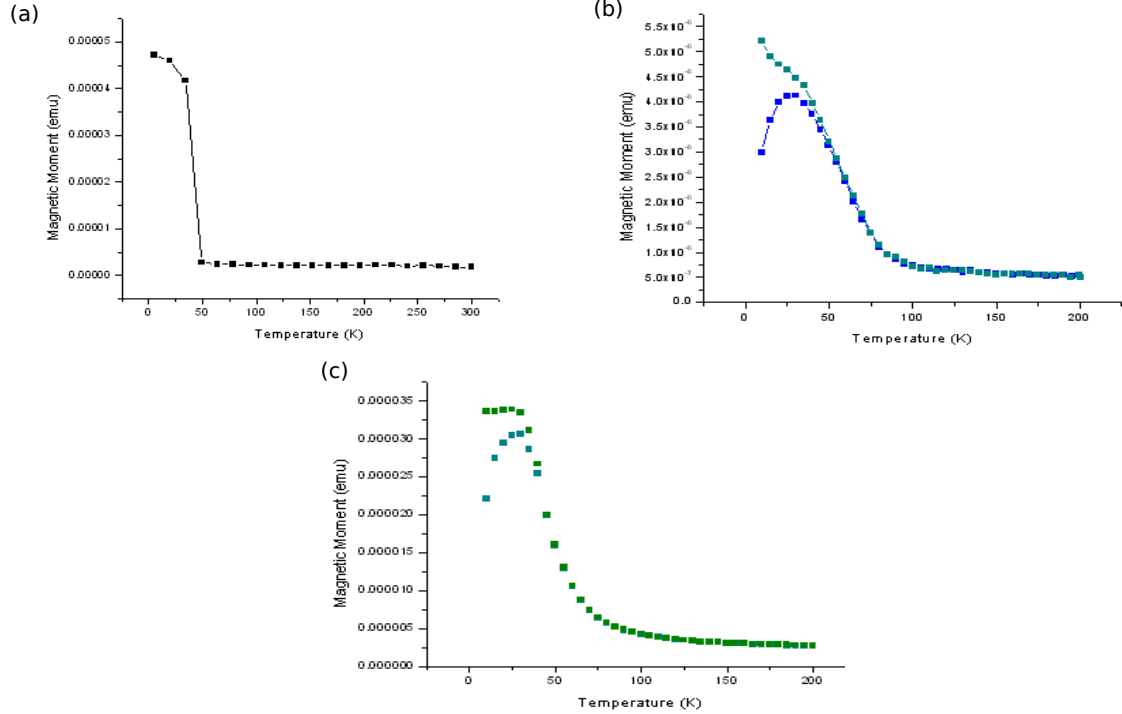


Figure 8: M-T curves for (a) an unknown manganite, (b) sample 062608a of BiMnO<sub>3</sub>, and (c) sample 062708a of BiMnO<sub>3</sub>.

In contrast to the steep drop for sample 010708a, the  $T_C$  curves for samples 062608a and 062708a are very gradual. This result is consistent with published literature on thin films of BiMnO<sub>3</sub> (see [1]). The cause of this gradual slope in the M-T curve is not understood, and inhibits accurate determination of the  $T_C$  for BiMnO<sub>3</sub>. An alternate, although less conventional way, to determine the  $T_C$  of a material is to identify the temperature at which the coercive field goes to 0. Figure 9 shows the plot of the coercive field with respect to temperature for sample 071508a, along with the tangent line used to extrapolate the temperature at which the coercive field would be 0. The  $T_C$  for sample 071508a of BiMnO<sub>3</sub> is approximately 93 K, which is slightly below the published literature indicating a  $T_C$  of 100-105 K (see [1]).

The  $T_C$  for sample 062708a (grown at 650 K) is approximately 60 K, which is less optimal

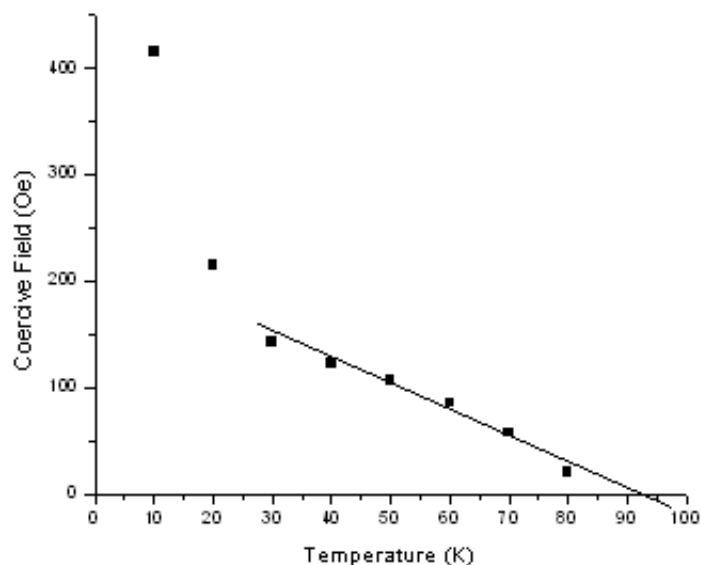


Figure 9: The coercive field of sample 062708a with respect to temperature. The tangent line indicates that the coercive field would go to 0 at approximately 93 K.

that the value of 90 K determined for the sample 062608a (grown at 600 K). This result led to the conclusion that the optimal growth temperature for  $\text{BiMnO}_3$  is around 600 K, but less than 650 K. The preceding sample 071508a, deposited at 620 K, showed a  $T_C$  of 93 K, as described above. Thus, the optimal growth temperature of  $\text{BiMnO}_3$  has been determined to be 620 K.

### 4.3 Magnet System

I used a 9-T superconducting magnet system from American Magnetics was used to analyze the resistance of the samples over a range of temperatures. I regulated the temperature with a Janis SuperVaritemp insert. The temperature was varied from 200 to 300 K, and the resistivity was determined using the 2-probe method, illustrated in Fig. 10. The 2-probe method must be used because the sample has very high resistivity, such that the resistance of the voltmeter is comparable to that of the sample. The comparable resistances cause a significant fraction of the current to pass through the voltmeter (and not through the sample), resulting in inaccurate voltage readings across the sample.

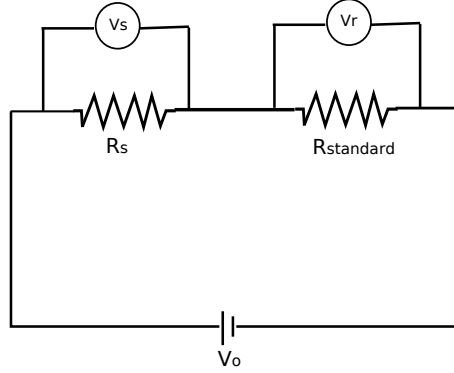


Figure 10: Illustration of the 2-probe method of measuring the resistance of a highly resistive sample.

The plot shown in Fig. 11 was generated by the Labview data collection program and shows the sheet resistance versus temperature for sample 062608a. The temperature was ramped from 200 to 300 K and then returned to 200 K. The sheet resistance is at a minimum of  $1.88 \times 10^4 \Omega$  at 300 K and a maximum of  $2.55 \times 10^6 \Omega$  at 198 K. The sheet resistance is a measure of the resistance of a thin film of uniform thickness. A high resistance is necessary for a ferroelectric material because a conductor cannot sustain an electric field.

#### 4.4 Atomic Force Microscopy

I used Atomic force microscopy (AFM) to determine the thickness and topography of the  $\text{BiMnO}_3$  thin films. Etching is performed to determine the thickness of the film. This is a destructive process whereby a chemical removes a portion of the film from a partially exposed sample, leaving an edge between the film and the substrate, as seen in Fig. 12a. As the tip of the AFM probe scans the surface, it records the height of the sample, thus giving the difference in height between the substrate and the film along the etched boundary. The thickness of our  $\text{BiMnO}_3$  films deposited for 40 min is 297.34 nm.

AFM was also used to show the topography of our  $\text{BiMnO}_3$  thin films. We employed the “tapping mode” in which the cantilever oscillates up and down near its resonance frequency. The amplitude of the oscillation decreases when the probe is close to the sample as a result

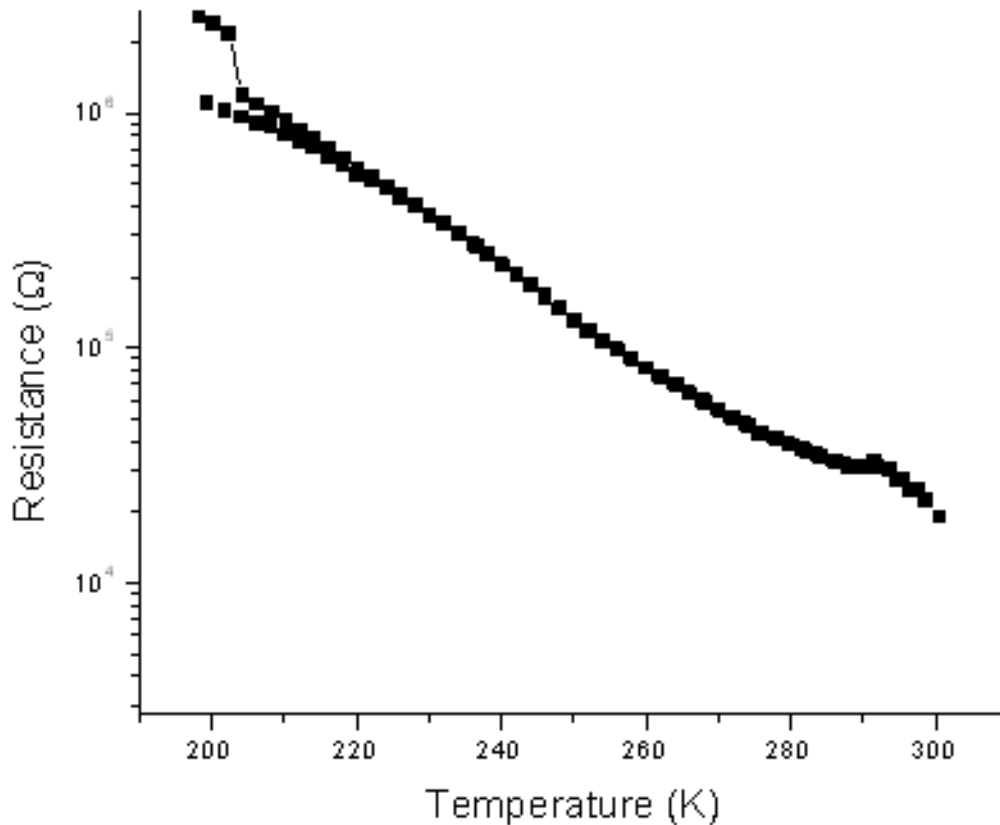


Figure 11: Plot of the sheet resistance versus temperature for sample 062608a, showing high resistivity and insulating properties.

of dipole-dipole, Van der Waals, electrostatic, etc, interactions. By imaging the force of the contact between the sample surface and the tip, the image shown in Fig. 12(b) is generated. This image of the topography of BiMnO<sub>3</sub> thin film is 4 μm in width and shows that the film deposited through island growth. Island growth occurs when atoms deposit on the substrate in patches, and many “islands” form and grow independently before coming together to form the overall film.

## 5 Conclusions

The properties of thin-film BiMnO<sub>3</sub> are very sensitive to growth conditions that affect not only the T<sub>C</sub> and the coercive field, but also the purity of the sample itself. BiMnO<sub>3</sub> is

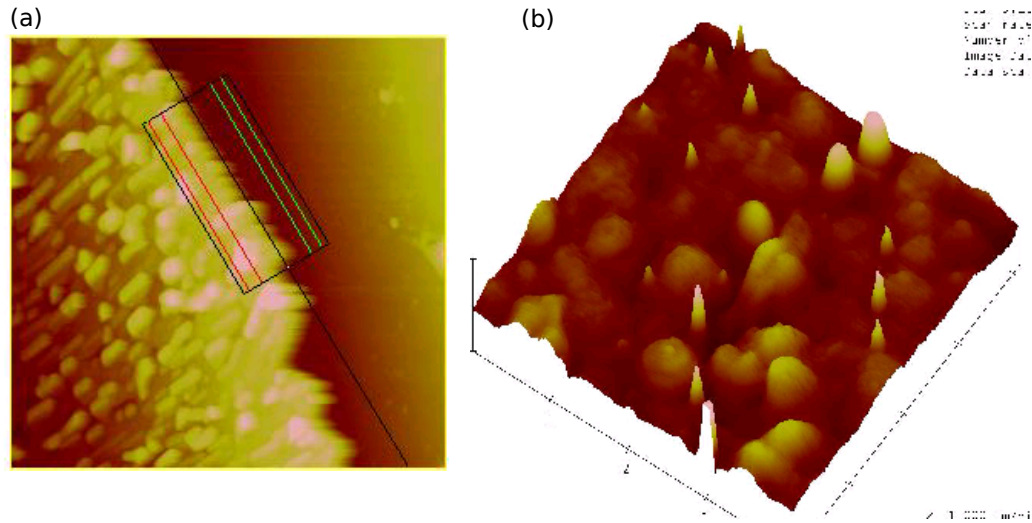


Figure 12: Image (a) shows the step between the film and the substrate, indicating a film thickness of 297.34 nm and image (b) shows the topography of the thin film indicating island growth

synthesized at temperatures below 650 °C, while a different manganite is more stable at higher temperatures. Fujino et. al. suggest this alternate manganite is  $\text{Mn}_3\text{O}_4$  [1]. The  $T_C$  was optimized at approximately 93 K at a growth temperature of 620 K and an oxygen partial pressure of 25 mTorr. The coercive field at these conditions was 420 Oe at 10 K.

Further investigation into the properties of  $\text{BiMnO}_3$  is needed to fully understand the electrical and magnetic properties of this multiferroic material. In particular, the study of strain effects may lead to a better understanding of magnetoelectric coupling in  $\text{BiMnO}_3$ , as well as a possible means to enhance and take advantage of it for technological ends.

## 6 Acknowledgments

I would like to acknowledge the UF Physics program and the NSF for this REU experience. I would also like to thank Art Ianuzzi for his assistance. And finally, thanks to Dr. Amlan Biswas for his guidance throughout this project and for all the coffee.

## References

- [1] S. Fujino., M. Murakami, S. H. Lim, L. G. Slamanca-Riba, M. Wuttig, and I. Takeuchi, *J. Appl. Phys.* **101**, 013903 (2007).
- [2] W. Eerenstein., F. D. Morrison, J. F. Scott, and N. D. Mathur, *Appl. Phys. Lett.* **87**, 101906 (2005).
- [3] W. Prellier, M. P. Singh, and P. Murugavel., *J. Phys.: Condens. Matter* **17**, R803-R832 (2005).
- [4] M. Dawber, K. M. Rabe, and J. F. Scott, *Rev. Mod. Phys.* **77**, 1083-1124 (2005).